buildings

MDPI

Article

The Utilization of Crushed Corn Cob as a Sand Substitute in Portland Cement Mortars for Sustainable Construction

Ana Torre *, Sorin Ramirez *, Isabel Moromi, Ladislao Basurto and Carmen Reyes

Faculty of Civil Engineering, National University of Engineering, Lima 150128, Peru; imoromi@uni.edu.pe (I.M.); jbasurto@uni.edu.pe (L.B.); carmenreyespe@yahoo.es (C.R.)
* Correspondence: anatorre@uni.edu.pe (A.T.); sorin.ramirez.c@uni.pe (S.R.)

Abstract: The utilization of mineralized sandy shredded corn cob (SCC) as a partial replacement for fine aggregate in Portland cement mortars (PM) presents an innovative opportunity for sustainable construction and organic waste reutilization. This study aims to assess the impact of SCC, with granulometric variations G1 and G2, on eight mortar formulations (PM, SCC-G1-5%, SCC-G1-10%; SCC-G2-5%, SCC-G2-10%, SCC-G2-15%, SCC-G2-20%, and SCC-G2-30%) with a consistent water-to-cement ratio of 0.55. Fresh-state properties (flowability, temperature, pH, unit weight, and setting time) and hardened-state characteristics (compressive strength at 4, 7, 14, and 28 days) were evaluated. Notably, flowability decreased by 90% for G2 designs with up to 15% SCC, unit weight decreased by up to 12% with SCC-G2-30%, setting time was delayed, and compressive strength for all SCC mortars up to 20% exceeded 21.9 MPa. In conclusion, the partial replacement of sand with a G2 particle-size distribution of SCC is feasible, with an optimal performance observed in SCC-G2-5%.

Keywords: corn cob; concrete; fine aggregate; compressive strength; granulometry

check for updates

Citation: Torre, A.; Ramirez, S.; Moromi, I.; Basurto, L.; Reyes, C. The Utilization of Crushed Corn Cob as a Sand Substitute in Portland Cement Mortars for Sustainable Construction. *Buildings* **2024**, *14*, 594. https://doi.org/10.3390/buildings14030594

Academic Editor: Rui Xiao

Received: 13 January 2024
Revised: 8 February 2024
Accepted: 21 February 2024
Published: 23 February 2024

Copyright: © 2024 by the authors. Licensee MDPI, Basel, Switzerland. This article is an open access article distributed under the terms and conditions of the Creative Commons Attribution (CC BY) license (https://creativecommons.org/licenses/by/4.0/).

1. Introduction

The global demand for sand and gravel in construction, which amounts to about fifty billion tons each year, is a major pollutant and causes flooding, the depletion of aquifers, and even worsens periods of drought [1].

In addition, sand mining is a catastrophic practice because it endangers natural ecosystems [2]. The environmental impacts of concrete can be significantly reduced by using organic wastes obtained from various industrial by-products [3] as a partial replacement for fine aggregate. Therefore, reducing quarrying activity is critical not only from an economic perspective, but also to preserve our ecosystem by mitigating the environmental threats to the atmosphere associated with the production of concrete components [4].

The trend of various research works has been to employ agricultural organic wastes [5] such as peanut shells as a replacement material for fine aggregate [6], oyster shell wastes (WOS) at 5% as a sand replacement for optimal use in construction [7], and the use of 70% of it in the replacement of granulated cork sand (CH70) in hydraulic mortar for the correction of thermal bridges [8].

This research will study corn cob, which is an agricultural waste by-product creating serious environmental problems during its generation and disposal [3], so finding a suitable use for these waste by-products as substitute construction materials is a promising area of research, as it could provide cost-effective [4,9], ecological, and sustainable solutions for the construction and waste-management sectors [5,10,11]. Furthermore, it is known that Peru is considered to be the center of origin of maize, with maize being the most important crop in extension for Peru [12].

The ear has evolved from a panicle to become a complex structure capable of harboring multiple kernels with abundant nutrient reserves [13]. This leads to the fact that the cob, and the multiple tissues that compose it as a whole, can be considered a potential resource in the

field of construction; for example, its use in the stabilization of soils with percentages of 20% to 50% of CCA due to the increase in compressive strength, resistance, and durability [10].

Corn starch mixed with water and cement was even used to create a material with moderate resistance, but with deficiencies in durability and sustainability that make its commercial use difficult [14]. In addition, corn cob can also be used as a coarse aggregate to prepare a low-carbon green recycled concrete (LCRC), obtaining promising results by reducing carbon emissions by up to 31% compared to common cement [15]. Similarly, corn ash was used as a partial replacement of sand in concrete due to natural resource depletion with promising results [16].

Currently, the vast majority of research [3] focuses on the use of corn cob ash (CCA) as a replacement for Ordinary Portland Cement (OPC) in order to study its influence on the various physical [17] and mechanical properties of concrete: water absorption, porosity [18], compressive strength [4,10,17], tensile strength [4], flexural strength [3,17] and durability [3,9].

Chemical properties were also of great interest, where several investigations showed that the addition of corn cob ash (CCA) increases the resistance against chemical attacks by chlorides and sulfates with 15% CCA content [9,19]. However, there are adverse effects such as a decrease in permeability, as well as a reduction in weight loss due to the reaction of the samples with HCl and acidic water H 2 SO 4 [9].

Corn ash as an admixture is effective for the long-term strength development of concrete, but its initial strength development is very slow [11]. CCA can be used when compressive strength is required, but not as more than a 10% replacement [20,21]. Therefore, recent studies sought ways to accelerate early strengths with nanosilica (NS), with up to 2% NS being of an optimal value to improve the early strength development of concrete with 10% CCA [11]. Similarly, 10 % CCA mixed with silica fume was found to increase compressive and tensile strength [21].

Other studies focus on the study of the thermal properties of CCA, which, when incorporated in the replacement of OPC, has insulating properties [18,20,22].

Some studies indicate that untreated corn ash is not shown to be a promising pozzolanic material due to its low pozzolanic activity, but to be an inert one. It may even have a negative impact on concrete performance [23].

However, a concrete with corn treated with cement paste (TCCA) to improve cement compatibility can be used for up to 40% sand replacement in concrete for the construction of lighter structures [2], an important gain from the point of view of the seismic behavior of buildings [17].

Another more viable alternative to manage large quantities of these materials could be their application in low-strength projects, as fillers or in the production of blocks [23] However, it can be used in non-structural application, as done in pavement regularization layers [22].

In summary, it has been noted that several studies have been conducted on ashes from corn cob. However, there is little documented information on the treatment and use of mineralized sandy shredded corn cob (SCC) as a substitute for fine aggregate in mortar formulation. Therefore, the objective of this paper is to evaluate the effect of using SCC as a partial replacement of fine aggregate in Portland cement mortars. The importance of this research lies in its potential to promote the use of environmentally friendly materials in construction in Peru and worldwide.

2. Materials and Methods

According to the flow diagram presented in Figure 1, first the properties of the natural sand were determined: fineness modulus, moisture, absorption, and specific weight. The crushed corn cob was mineralized and its characteristics were described with a mixture of cement and water in order to be used as a replacement for sand in the mix, and was designed using two different granulometries of SCC and water–cement ratio of 0.5. In addition, the internal structure and chemical composition of the corn particles were studied

using Scanning Electron Microscopy (SEM). The mix designs were made based on the ACI 211 limit based on the two required particle sizes. Finally, a series of tests were performed on both fresh and hardened concrete specimens to investigate the physical and mechanical properties of the mortar with different contents and particle sizes of mineralized corn cob.

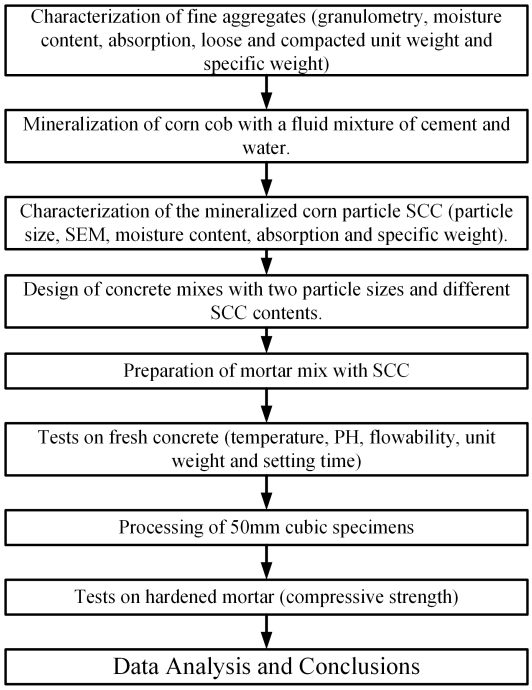


Figure 1. The flowchart of the methodology.

2.1. Untreated Shredded Corn Cob

The cob is composed of a central core of large parenchyma cells, whose role is to store nutrients [13]. In addition, it is composed of cellulose fibers, hemicellulose, and lignin in the pith, and the woody ring and glume are different, which indirectly affects the mechanical properties of the corn cob. [24]. Among them, we highlight lignin, which is a filler and binder substance of the fiber skeleton, being an important source of cellular strength and structural toughness, which can improve the mechanical properties of corn cob [25].

In this research, maize cob, also known as corn cob, presents a fibrous structure, rough texture, light weight, and a golden or light brown color, as observed in Figure 2. In addition, it is spongy and porous with small dimples, and the density is found to be approximately 170 kg/m^3 to 295 kg/m^3 [26].



Figure 2. Non-mineralized dried shredded corn cob.

2.1.1. Mineralization with a Cement–Water Mixture

For use in this research, the maize cob sample was reduced in size to obtain particles with two different particle granulometries (G1 and G2), as shown in Figure 3. These were exposed to the environment for 12 h and then subjected to a drying process in an oven at a temperature of 98 °C ± 2 °C for six hours, until they reached a constant weight.

Subsequently, mineralization was carried out by immersing the crushed corn in a fluid mixture of cement and water with a volumetric ratio of 1:3. Then, they were mixed using manual concrete-mixing equipment for 5 min in a container of approximately 10-liter volume until the specific surface area of the particles was completely covered.

Finally, the mixture was poured into a container and left to dry for about 30 min. Afterwards, the material was placed in a small mixer without water and mixed for 5 min at 40 RPM constantly, thus achieving the dispersion of SCC.



(**a**) (**b**)

Figure 3. Mineralized SCC with various granulometries. (**a**) Mineralized SCC with particle size G1. (**b**) Mineralized SCC with particle size G2.

2.1.2. The Granulometry of the SCC

Table 1 shows the size distribution of the G1 particles of the SCC, with a predominant size in the No. 8 mesh (2.36 mm), which is equivalent to a cumulative retained percentage of 96.57% and a fineness modulus (FM) equal to 4.9.

Table 1. SCC particle-size distribution G1.

Sieve #	Retained Weight	%Retained Weight	%Accumulated Retained Weight	%Passing
3/8"	0.00	0.00	0.00	100.00
4	1.80	0.60	0.60	99.40
8	287.90	95.97	96.57	3.43
16	6.60	2.20	98.77	1.23
30	1.00	0.33	99.10	0.90
50	0.30	0.10	99.20	0.80
100	0.20	0.07	99.27	0.73
200	2.20	0.73	100.00	0.00

Table 2 shows the size distribution of the G2 particles' distribution for the SCC, with a predominant size on the No. 16 mesh (2.36 mm), which is equivalent to an accumulative retained percentage of 60.17% and a fineness modulus (FM) equal to 3.12.

Figure 3 shows the particle dimensions for G1 and G2. In addition, both samples are irregular in shape with angular edges and rough textures, very similar to that of a natural sand particle. Figure 4 shows the different sizes of the G2 granulometry sample studied.



Figure 4. Grain-size distribution of mineralized SCC G2.

Table 2. SCC particle-size distribution G2.

Sieve #	Retained Weight	%Retained Weight	%Accumulated Retained Weight	%Passing
3/8"	0.00	0.00	0.00	100.00
4	4.70	1.57	1.57	98.43
8	64.00	21.33	22.90	77.10
16	111.80	37.27	60.17	39.83
30	79.30	26.43	86.60	13.40
50	29.20	9.73	86.33	3.67
100	7.40	2.47	98.80	1.20
200	3.60	1.20	100.00	0.00

2.1.3. The Physical Properties of SCC

A summary table containing data on the main physical properties of SCC for both particle-size distributions and the standard method employed is presented in Table 3 below.

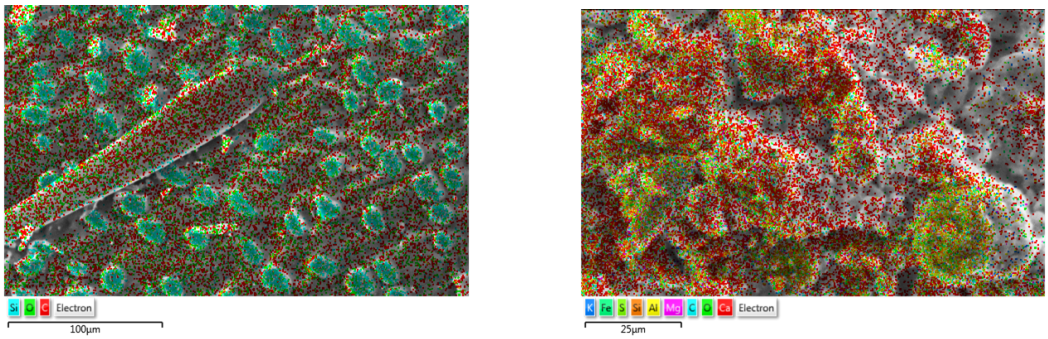
Table 3. Physical properties of SCC (G1 and G2).

Physical Properties	Unit	G1	G2	Method
Loose unit weight	kg/m^3	225	250	ASTM C29 [27]
Compacted unit weight	kg/m^3	240	275	ASTM C29
Specific gravity	kg/m^3	400	403	ASTM C128 [28]
Finesse modulus	dimensionless	4.94	3.12	ASTM C136 [29]
Absorption	%	180	170	ASTM C128
Moisture content	%	17	15	ASTM C566 [30]
Porosity	%	44.3	41	ASTM C29

2.1.4. SEM Microscopy of SCC

SEM imaging allows for the detection of SCC components with higher contrast and spatial resolution than optical approaches for compositional analysis and imaging [3].

Figure 5 shows the scanning electron microscopy (SEM) where the shape and size of the SCC particles can be appreciated. Figure 5a corresponds to unmineralized SCC (M1) and Figure 5b to mineralized SCC (M2).



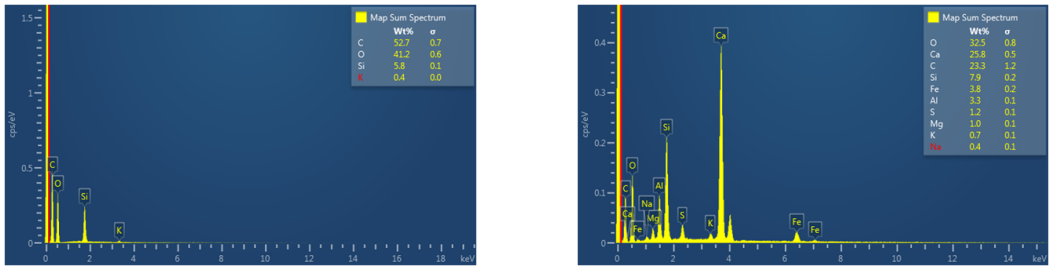
(**a**) (**b**)

Figure 5. Microscopy of the SCC with G2 granulometry. (**a**) Sample M1 unmineralized. (**b**) Sample M2 mineralized.

Figure 5a,b show the increase in density when the SCC particles are mineralized, and the porosity on the surface of the mineralized particles is reduced. Additionally, the unmineralized SCC has silicon (Si), oxygen (O), and carbon (C) in its matrix, while the mineralized SCC sample with cement slurry contains potassium (K), iron (Fe), sulfur (S), silica (Si), aluminum (Al), magnesium (Mg), carbon (C), oxygen (O), and calcium (Ca).

2.1.5. X-ray Spectrometry

By means of X-ray diffraction analysis, the main chemical elements that compose the SCC were identified and are shown in the diafractograms in percentage by weight in Figure 6, where M1 and M2 correspond to the nomenclature used in SEM.



(**a**) (**b**)

Figure 6. Diffractogram of the SCC with G2 granulometry (**a**) Sample M1 unmineralized. (**b**) Sample M2 mineralized.

The X-ray diffractogram in Figure 6 reveals the chemical composition in weight percentages of the SCC: 32.5% oxygen (O), 25.8% calcium (Ca), 23.3% carbon (C), 7.9% silica (Si), 3.8% iron (Fe), and 3.3% aluminum (Al), i.e., the sample is most likely composed of some mineralogical series of aluminates, silicates, and oxides. In addition, Pinto [26] reported very similar values for the chemical composition of the SCC.

2.2. Portland Cement Type I

The cement used was Portland Type I, which complies with ASTM C150 [31].

2.3. Fine Aggregate

The fine aggregate is of natural origin, coming from the Jicamarca quarry in Lima, Peru.

Physical Properties

The particle size was evaluated according to ASTM C136 [29] for fine aggregates. Table 4 shows the granulometric analysis of the sand used; the fineness modulus obtained was equal to 2.51.

Table 4. Granulometric analysis of the fine aggregate.

Sieve #	Retained Weight	%Retained Weight	%Accumulated Retained Weight	%Passing
3/8"	0.00	0.00	0.00	100.00
4	6.40	1.07	1.07	98.93
8	99.30	16.54	17.61	82.39
16	94.10	15.68	33.29	66.71
30	86.40	14.40	47.68	55.32
50	114.30	19.04	66.73	33.27
100	98.80	16.46	83.19	16.81
200	100.90	16.81	100.00	0.00

Table 5 below summarizes the main characteristics of the fine aggregate.

Table 5. Summary of physical properties of the fine aggregate.

Physical Properties	Unit	Value	Method
Loose unit weight	kg/m^3	1649	ASTM C29 [27]
Compacted unit weight	kg/m^3	1882	ASTM C29
Specific gravity	kg/m^3	2639	ASTM C128 [28]
Finesse modulus	dimensionless	2.50	ASTM C136 [29]
Absorption	%	0.82	ASTM C128
Moisture content	%	1.09	ASTM C566 [30]

2.4. Superplasticizer Additive

The superplasticizer additive used complies with ASTM C494 [32] , and is classified as Type F. It has a liquid appearance being opalescent white in color with a density equal to 1.1 g/mL.

2.5. Experimental Program

2.5.1. Concrete Mix Design

Table 6 shows eight mortar dosages, including the standard mortar (PM). For all cases, a water/cement (w/c) ratio of 0.55 was maintained, and sand substitutions were carried out with SCC in volumetric proportions of 5%, 10%, 15%, 20%, and 30% of the natural sand volume. In addition, the two fine-aggregate granulometries G1 and G2 of SCC were used.

Table 6. Mortar dosage with 0%, 5%, 10%, 15%, 20%, and 30% of SCC for 1 m^3.

Material	Unit	PM	SCC-G1-5% SCC-G2-5%	SCC-G1-10% SCC-G2-10%	SCC-G2-15%	SCC-G2-20%	SCC-G2-30%
Cement	kg	450	450	450	450	450	450
Water	kg	243	244	244	244	244	244
Air	kg	0	0	0	0	0	0
Sand	kg	1536	1459	1382	1310	1245	1190
Cob	kg	0	25	50	75	100	150
Additive	g	2	2	2	2	2	2

2.5.2. The Production of Cubical Mortar Specimens

The mortar mixture is prepared according to ASTM C305 [33], using a 4-liter container mixer. In the mortar-mixing process, the SCC particles were incorporated simultaneously with the fine aggregate. Subsequently, cubic specimens of mortar 50 mm on each side were molded according to ASTM C109 [34] . For each design, 12 cubes were molded, making a total of 96 samples. The specimens were left inside the molds for 24 h, after which they were removed and cured in alkaline water (3 g of lime per liter) for proper hydration for 3, 7, 14, and 28 days as shown in Figure 7.



(**a**) (**b**) (**c**)

Figure 7. Mortar-sample-processing sequence: (**a**) Molding. (**b**) Demolding. (**c**) Curing.

2.6. Testing Methods

2.6.1. The Flow of the Hydraulic Cement Mortar

The flowability of the mortar was evaluated according to ASTM C1437-20 [35], using a shaking table. This was done for each of the eight mix designs, as shown in Figure 8. The average initial and final diameters of the mortars were recorded.



(**a**) (**b**) (**c**)

Figure 8. Fluidity of mortars. (**a**) PM. (**b**) SCC-G1-5%. (**c**) SCC-G1-10%.

2.6.2. The Unit Weight of Mortar

The unit weights were determined for the eight types of mortar according to ASTM C138 [36]. Figure 9 shows the weights obtained for the different types of mortar tested.



(**a**) (**b**) (**c**)

Figure 9. Mortar unit weights. (**a**) PM. (**b**) SCC-G1-5%. (**c**) SCC-G1-10%.

2.6.3. The Setting Time of Mortar

The setting time was determined using the ASTMC403/403M [37] with a Penetrometer needle, as shown in Figure 10a, from a sample of fresh mortar placed in a container at a temperature between 20 to 25 °C. The needle was then introduced at regular intervals to measure the penetration resistance of the mortar, as shown in Figure 10b. The finalized test is shown in Figure 10c. Additionally, the initial and final setting time was determined, and the corresponding graphs were plotted.



(**a**) (**b**) (**c**)

Figure 10. The setting time for the SCC-G2-10% mortar. (**a**) Penetrometer. (**b**) Needle penetration into the mortar. (**c**) Tested sample.

2.6.4. The Temperature and PH of the Mortar

Temperature was measured using ASTM C1064 [38] and PH was measured using ASTM D4262 [39] method for the eight types of mortars, obtaining values between 24.2 °C and 24.5 °C; similarly, PH in all cases was alkaline between 12.3 and 12.5. These results are slightly below those obtained with CCA [18]. Figure 11 shows these tests.



Figure 11. Temperature and PH of the mortars with SCC.

2.6.5. The Compressive Strength of Mortar

Sixty cubic samples of mortars were tested according to ASTM C109/C109M [34], at curing ages of 4, 7, 14, and 28 days, as shown in Figure 12.



(**a**) (**b**) (**c**)

Figure 12. Compressive strength test. (**a**) Versa-Tester testing machine. (**b**) Test. (**c**) Specimen tested.

3. Results and Discussions

3.1. Mortar Flowability

The results of the flowability of the mortar are presented in Table 7, where a considerable decrease in the flowability of the mortars with SCC-G1 was observed, even reaching only 54.50% of the flowability of the PM, while the mortars with SCC-G2 with 5%, 10%, and 15% presented a flowability between 90% and 99% of that of the standard mortar (PM).

Table 7. Mortar diameter and flowability with CSS.

Design	Average Diameter (cm)	Fluidity (%)
PM	20.10	100.00
SCC-G1-5%	16.90	69.00
SCC-G1-10%	15.45	54.50
SCC-G2-5%	19.93	99.30
SCC-G2-10%	19.40	93.04
SCC-G2-15%	19.20	91.05
SCC-G2-20%	18.00	79.10
SCC-G2-30%	17.00	69.15

An important factor in flowability was the particle shape of the SCC, since mortars with rounder aggregates (G1 particle size) produce higher workability, while elongated particles (G2 particle size) cause higher friction and reduced workability [2]. In addition, the decrease in workability as observed in Figure 8 is due to water absorption by the higher amount of cob in the mixture and would have the same behavior as corn ash [3,4,10].

The flowability of the mortar was negatively affected by the increase in the amount of SCC. This phenomenon was influenced both by the morphology of the SCCs as well as by their high water-absorption capacity, which reduced the flowability of the mixture, even when maintaining constant w/c values.

In addition, corn cob is known to be composed of cellulose, hemicellulose, lignin, pectin, and waxes, and could have an inhibitory effect on cement hydration [2].

3.2. The Unit Weight of Mortar

Table 8 shows the unit weight per cubic meter, corresponding to the eight types of mortars evaluated with SCC, following the ASTM C138 [36]. The highest unit weight of 2214 kg/cm^3 was obtained with the PM design and the lowest of 1946 kg/cm^3 with SCC-G2-30%. The decrease in unit weight is due to the replacement of SCC [2], which has a lower density than fine aggregate [3,4,16].

Table 8. Unit weight of mortar with SCC in fresh state.

Design	Unit Weight (kg/m^3)	% Unit Weight with Respect to the PM
PM	2214	100
SCC-G1-5%	2154	97
SCC-G1-10%	2102	95
SCC-G2-5%	2030	92
SCC-G2-10%	2010	91
SCC-G2-15%	1990	90
SCC-G2-20%	1951	88
SCC-G2-30%	1946	88

The results show in all cases a decrease in the unit weight of the mortar with respect to PM when replacing up to 30% of the fine aggregate with both particle sizes (G1 and G2).

3.3. The Setting Time of Mortar

Applying the ASTM C403/C403M [37], the setting time of the mortar with the addition of SCC was determined for SCC-G2-5% and SCC-G2-10%, because these had the best

performances in flowability, workability, and resistance from the eight studied designs as per Table 7. The initial setting was observed at 119 min, and the final setting occurred at 155 min for the standard mortar (PM). For the SCC-G2-5% and SCC-G2-10% designs, the initial setting times were 135 and 168 min, respectively. Additionally, the final setting times for these two designs were 184 and 215 min, respectively. It is noted that the setting time increased with the introduction of SCC, as shown in Figure 13, due to the slower response compared to cement hydration [3].

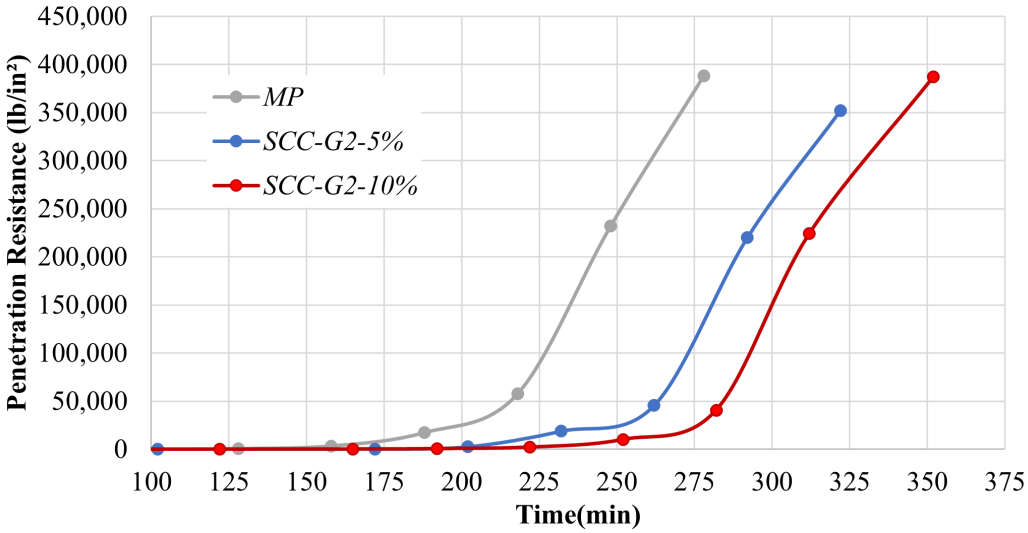


Figure 13. Setting times for standard mortar (PM), SCC-G2-5%, and SCC-G2-10%.

3.4. Compressive Strength

Table 9 shows the compression results of the eight mortar mixes at curing ages of 3, 7, 14 and 28 days. In the PM control samples, the fastest rates of early strength development were recorded, with maximum strengths of 37.1 MPa being reached at 28 days of curing, while the lowest strengths were obtained with SCC-G2-30% for all curing ages.

Table 9. Compressive strength in MPa at ages of 3, 7, 14, and 28 days of curing.

Design	3 Days	7 Days	14 Days	28 Days
PM	24.8	28.9	33.3	37.1
SCC-G1-5%	21.7	25.0	22.9	26.5
SCC-G1-10%	18.7	12.3	15.3	21.2
SCC-G2-5%	18.8	22.2	28.5	31.0
SCC-G2-10%	14.7	18.8	23.0	26.9
SCC-G2-15%	13.2	17.2	20.6	23.5
SCC-G2-20%	12.4	16.3	19.1	21.9
SCC-G2-30%	10.3	13.4	16.2	18.1

The data indicate that the age of the mortar and the proportion of SCC are significant factors in the strength of the material. In addition, the finer the particle size of the SCC aggregate, i.e., with G2, the better the results obtained at 28 days of curing [2] as shown in Figure 14.

From Table 9, it is concluded that SCC can be used when compressive strength is required, but not for more than a 20% replacement for structural concrete.

The results showed that the compressive strength increases with the curing age and decreases with increasing SCC content in the mix [16,20]; similar results are obtained when it is replaced with CCA [4,10,17].

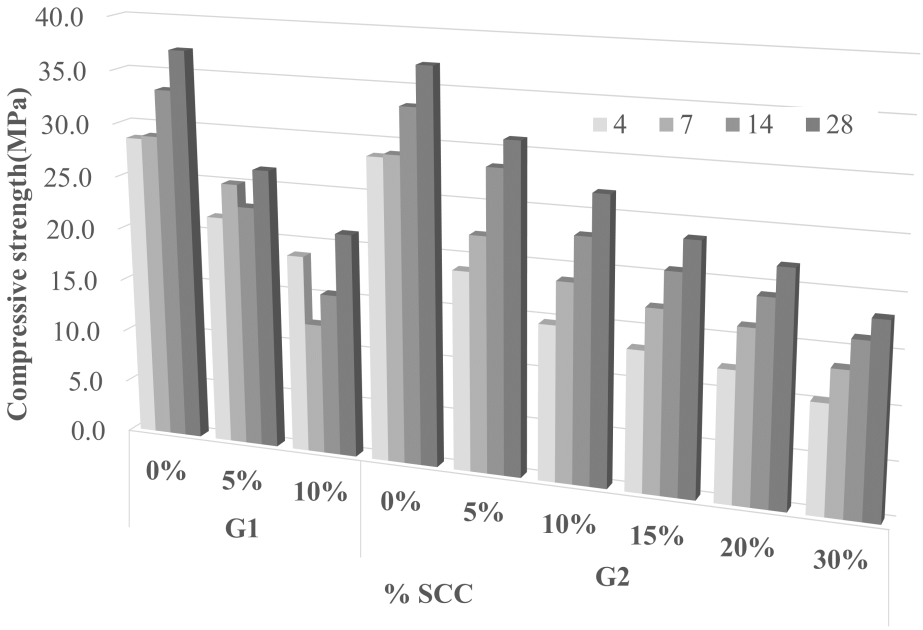


Figure 14. Compressive strength of mortar at curing ages of 4, 7, and 14 days.

4. Conclusions

From the analysis of the results obtained in this study, the following conclusions were reached:

- It is feasible to use SCC as a substitute for natural fine aggregate, ensuring a G2 granulometry of FM 3.12, and wet curing times equal to 28 days;
- Through SEM and spectrometry analysis, it was demonstrated that the mineralization process applied to the SCC by adding cement slurry improved the properties of the SCC matrix used in the mix design;
- By comparing the compressive strength results of mortars with G1 and G2 granulometries, it is concluded that samples with G2 achieved higher resistances;
- The flowability of the mortar was slightly affected for samples with up to 15% SCC and G2 granulometry. However, it decreased significantly to approximately 54.50% with G1 granulometry;
- A 12% reduction in the unit weight of the mortar was achieved by replacing 30% of the fine aggregate with SCC;
- The setting time of mortar mixtures with SCC in amounts of 5% and 10% with G2 delays the setting time in comparison to that of the standard mortar (PM);
- This solution led to a reduction in the consumption of up to 350 kg of natural sand per 1 m^3 of mortar;
- For the five designs with a G2 granulometry of SCC, strengths of up to 31.0 MPa were achieved with a 5% partial replacement of fine aggregate, and the lowest resistance was 18.1 MPa with 30% SCC. This signifies that we can achieve designs with structural strengths using lower contents of natural aggregates.

Author Contributions: A.T.: Conceptualization, methodology, investigation, data analysis, drafting, review and editing; S.R.: Investigation, data analysis, draft writing and editing; I.M.: Writing, editing and review; L.B.: Supervision, software, data curation and review; C.R.: Investigation, writing, editing and review. All authors have read and agreed to the published version of the manuscript.

Funding: This research received no external funding.

Data Availability Statement: Additional data will be available upon request. The data are not publicly available due to privacy.

Acknowledgments: We would like to express our gratitude to the Vice-Rectorate of Research of UNI for their invaluable support in carrying out this study. We would also like to thank the Laboratorio de Ensayo de Materiales (LEM UNI) of the Facultad de Ingeniería Civil (FIC) for the facilities provided for carrying out the tests.

Conflicts of Interest: The authors declare no conflicts of interest.

References

1. "La Explotación Insostenible de Arena Destruye ríOs y Mares", Noticias ONU. Available online: https://news.un.org/es/story/2019/05/1455611 (accessed on 26 November 2023).
2. Shao, K.; Du, Y.; Zhou, F. Feasibility of using treated corn cob aggregates in cement mortars. *Constr. Build. Mater.* **2021**, *271*, 121575. [CrossRef]
3. Ahmad, J.; Arbili, M.M.; Alabduljabbar, H.; Deifalla, A.F. Concrete made with partially substitution corn cob ash: A review. *Case Stud. Constr. Mater.* **2023**, *18*, e02100. [CrossRef]
4. Bheel, N.; Ali, M.O.A.; Liu, Y.; Tafsirojjaman, T.; Awoyera, P.O.; Sor, N.H.; Romero, L.M.B. Utilization of corn cob ash as fine aggregate and ground granulated blast furnace slag as cementitious material in concrete. *Buildings* **2021**, *11*, 422. [CrossRef]
5. Prusty, J. K.; Patro, S.K.; Basarkar, S. Concrete using agro-waste as fine aggregate for sustainable built environment—A review. *Int. J. Sustain. Built Environ.* **2016**, *5*, 312–333. [CrossRef]
6. Usman, J.; Pindiga, N.Y.; Mazizah, E. M.Influence of groundnut shell ash on the properties of cement pastes. *IOP Conf. Ser.* **2019**, *601*, 012015. [CrossRef]
7. Kuo, W.; Wang, H.; Shu, C.; Su, D. Engineering properties of controlled low-strength materials containing waste oyster shells. *Constr. Build. Mater.* **2013**, *46*, 128–133. [CrossRef]
8. Brás, A.; Gonçalves, F.V.; Faustino, P.M.Cork-based mortars for thermal bridges correction in a dwelling: Thermal performance and cost evaluation. *Energy Build.* **2014**, *72*, 296–308. [CrossRef]
9. Adesanya, D.; Raheem, A.A. A study of the permeability and acid attack of corn cob ash blended cements. *Constr. Build. Mater.* **2010**, *24*, 403–409. [CrossRef]
10. Adesanya, D. Evaluation of blended cement mortar, concrete and stabilized earth made from ordinary Portland cement and corn cob ash. *Constr. Build. Mater.* **1996**, *10*, 451–456. [CrossRef]
11. Oluremi, J.R.; Raheem, A.A.; Balogun, R.; Moshood, A. Early strength development assessment of concrete produced from cement replaced with nano silica activated Corn Cob Ash. *Mater. Today Proc.* **2023**, *86*, 36–40. [CrossRef]
12. "El Maíz es el Cultivo más Importante en Extensión para el Perú", Agraria.pe Agencia Agraria de Noticias. Available online: https://agraria.pe/noticias/el-maiz-es-el-cultivo-mas-importante-en-extension-para-el-pe-22033#:~:text=(Agraria.pe)%20El%20ma%C3%ADz,importancia%20socioecon%C3%B3mica%20para%20el%20pa%C3%ADs (accessed on 26 November 2023).
13. García-Lara, S.; Chuck-Hernandez, C.; Serna-Saldivar, S. Development and Structure of the Corn Kernel. In *Corn*; Elsevier: Amsterdam, The Netherlands, 2019; pp. 147–163. [CrossRef]
14. Kulshreshtha, Y.; Schlangen, E.; Jonkers, H.; Vardon, P.J.; Van Paassen, L.A. CoRncrete: A corn starch based building material. *Constr. Build. Mater.* **2017**, *154*, 411–423. [CrossRef]
15. Wang, P.; Liu, H.; Guo, H.; Yu, Y.; Guo, Y.; Yue, G.; Wang, L. Study on preparation and performance of alkali-activated low carbon recycled concrete: Corn cob biomass aggregate. *J. Mater. Res. Technol.* **2023**, *23*, 90–105. [CrossRef]
16. Memon, S.A.; Javed, U.; Khushnood, R.A. Eco-friendly utilization of corncob ash as partial replacement of sand in concrete. *Constr. Build. Mater.* **2019**, *195*, 165–177. [CrossRef]
17. Gradinaru, C.M.; Barbuta, M.; Babor, D.; Serbanoiu, A.A. Corn cob ash as sustainable puzzolanic material for an ecological concrete. *Bull. Transilv. Bras.* **2018**, *11*, 60. Available online: https://webbut.unitbv.ro/index.php/Series_I/article/view/2354/1872 (accessed on 12 January 2024).
18. Życiński, W.; Małek, M.; Jackowski, M.; Łasica, W.; Owczarek, M. Study of the workability and mechanical properties of concrete with added ground corncobs. *Mater. Tehnol.* **2020**, *54*, 479–483. [CrossRef]
19. Oyebisi, S.; Ede, A.N.; Olutoge, F.; Ogbiye, S. Evaluation of reactivity indexes and durability properties of slag-based geopolymer concrete incorporating corn cob ash. *Constr. Build. Mater.* **2020**, *258*, 119604. [CrossRef]
20. Oriola, K.O.; Raheem, A.A.; Ogundele, A. Investigation of compressive strength and thermal properties of corn cob ash cement concrete. *Mater. Today Proc.* **2023**, *86*, 128–133. [CrossRef]
21. Sharma, N.; Sharma, P.; Parashar, A.K. Incorporation of silica fume and waste corn Cob ash in cement and concrete for sustainable environment. *Mater. Today Proc.* **2022**, *62*, 4151–4155. [CrossRef]
22. Pinto, J.M.; Vieira, B.; Pereira, H.; Jacinto, C.; Vilela, P.; Paiva, A.; Varum, H. Corn cob lightweight concrete for non-structural applications. *Constr. Build. Mater.* **2012**, *34*, 346–351. [CrossRef]
23. Shakouri, M.; Exstrom, C.L.; Ramanathan, S.; Suraneni, P. Hydration, strength, and durability of cementitious materials incorporating untreated corn cob ash. *Constr. Build. Mater.* **2020**, *243*, 118171. [CrossRef]
24. Zou, Y.; Fu, J.; Chen, Z.; Liu, R. The effect of microstructure on mechanical properties of corn cob. *Micron* **2021**, *146*, 103070. [CrossRef] [PubMed]

25. Xu, F.; Zhong, X.; Sun, R.; Lu, Q. Anatomy, ultrastructure and lignin distribution in cell wall of Caragana Korshinskii. *Ind. Crops Prod.* **2006**, *24*, 186–193. [CrossRef]
26. Pinto, J.M.; Da Cruz, D.M.; Paiva, A.; Pereira, S.; Tavares, P.B.; Fernandes, L.; Varum, H. Characterization of corn cob as a possible raw building material. *Constr. Build. Mater.* **2012**, *34*, 28–33. [CrossRef]
27. *ASTM C29/C29M-23*; Standard Test Method for Bulk Density ("Unit Weight") and Voids in Aggregate. Annual Book of ASTM Standards. ASTM International: West Conshohocken, PA, USA, 2023.
28. *ASTM C128-22*; Standard Test Method for Relative Density (Specific Gravity) and Absorption of Fine Aggregate. Annual Book of ASTM Standards. ASTM International: West Conshohocken, PA, USA, 2022.
29. *ASTM C136/C136M-19*; Standard Test Method for Sieve Analysis of Fine and Coarse Aggregates. Annual Book of ASTM Standards. ASTM International: West Conshohocken, PA, USA, 2019.
30. *ASTM C566-19*; Standard Test Method for Total Evaporable Moisture Content of Aggregate by Drying. Annual Book of ASTM Standards. ASTM International: West Conshohocken, PA, USA, 2019.
31. *ASTM C150/C150M-22*; Standard Specification for Portland Cement. Annual Book of ASTM Standards. ASTM International: West Conshohocken, PA, USA, 2022.
32. *ASTM C494/C494M-19e1*; Standard Specification for Chemical Admixtures for Concrete. Annual Book of ASTM Standards. ASTM International: West Conshohocken, PA, USA, 2019.
33. *ASTM C305-20*; Standard Practice for Mechanical Mixing of Hydraulic Cement Pastes and Mortars of Plastic Consistency. Annual Book of ASTM Standards. ASTM International: West Conshohocken, PA, USA, 2020.
34. *ASTM C109/C109M-23*; Standard Test Method for Compressive Strength of Hydraulic Cement Mortars (Using 50 mm [2 in.] Cube Specimens). Annual Book of ASTM Standards. ASTM International: West Conshohocken, PA, USA, 2023.
35. *ASTM C1437-20*; Standard Test Method for Flow of Hydraulic Cement Mortar. Annual Book of ASTM Standards. ASTM International: West Conshohocken, PA, USA, 2020.
36. *ASTM C138/C138M-23*; Standard Test Method for Density (Unit Weight), Yield, and Air Content (Gravimetric) of Concrete. Annual Book of ASTM Standards. ASTM International: West Conshohocken, PA, USA, 2023.
37. *ASTM C403/C403M-23*; Standard Test Method for Time of Setting of Concrete Mixtures by Penetration Resistance. Annual Book of ASTM Standards. ASTM International: West Conshohocken, PA, USA, 2023.
38. *ASTM C1064/C1064M-23*; Standard Test Method for Temperature of Freshly Mixed Hydraulic-Cement Concrete. Annual Book of ASTM Standards. ASTM International: West Conshohocken, PA, USA, 2023.
39. *ASTM D4262-05(2018)*; Standard Test Method for pH of Chemically Cleaned or Etched Concrete Surfaces. Annual Book of ASTM Standards. ASTM International: West Conshohocken, PA, USA, 2018.

Disclaimer/Publisher's Note: The statements, opinions and data contained in all publications are solely those of the individual author(s) and contributor(s) and not of MDPI and/or the editor(s). MDPI and/or the editor(s) disclaim responsibility for any injury to people or property resulting from any ideas, methods, instructions or products referred to in the content.